

Optimal Receive Antenna Selection in Time-Varying Fading Channels with Practical Training Constraints

Vinod Kristem, Neelesh B. Mehta, *Senior Member, IEEE*, Andreas F. Molisch, *Fellow, IEEE*

Abstract—Hardware constraints, which motivate receive antenna selection, also require that various antenna elements at the receiver be sounded sequentially to obtain estimates required for selecting the ‘best’ antenna and for coherently demodulating data thereafter. Consequently, the channel state information at different antennas is outdated by different amounts and corrupted by noise. We show that, for this reason, simply selecting the antenna with the highest estimated channel gain is not optimum. Rather, a preferable strategy is to linearly weight the channel estimates of different antennas differently, depending on the training scheme. We derive closed-form expressions for the symbol error probability (SEP) of AS for MPSK and MQAM in time-varying Rayleigh fading channels for arbitrary selection weights, and validate them with simulations. We then characterize explicitly the optimal selection weights that minimize the SEP. We also consider packet reception, in which multiple symbols of a packet are received by the same antenna. New suboptimal, but computationally efficient weighted selection schemes are proposed for reducing the packet error rate. The benefits of weighted selection are also demonstrated using a practical channel code used in third generation cellular systems. Our results show that optimal weighted selection yields a significant performance gain over conventional unweighted selection.

Index Terms—Antenna selection, multiple antennas, diversity methods, fading channels, channel estimation, modulation schemes, channel coding, delays, training

I. INTRODUCTION

Antenna selection (AS) is a popular technique to reduce the hardware costs at the transmitter or receiver of a wireless system [1]–[7]. It uses fewer radio frequency (RF) chains than the actual number of antenna elements, and only processes signals from a dynamically selected subset of antennas. This is advantageous since antenna elements are typically cheap and easy to implement, while the RF chains are expensive. Consequently, many next generation standards such as IEEE 802.11n [8], Third Generation Partnership Project (3GPP) Long Term Evolution (LTE) [9], and the IEEE 802.16m Advanced WiMax [10] have standardized or are standardizing AS at the transmitter or the receiver, or both. In this paper, we concentrate on single receive antenna selection. While a receiver can have more RF chains, the model we consider is practically relevant and, as we shall see, analytically rich and

insightful. It achieves the same full diversity order as subset selection (with more RF chains) with perfect channel state information (CSI) [4], [11]–[14].

In practice, the CSI for receive AS, which is the focus of this paper, needs to be acquired using a pilot-based training scheme. The low hardware complexity, which is a key motivator for AS, imposes unique constraints on how training gets done for AS: given the limited number of RF chains, only one antenna can be activated at any instant. Consequently, the transmitter needs to send pilot(s) multiple times to enable the receiver to *sequentially* receive pilots with different antennas and estimate their corresponding links to the transmitter. The receive antenna is then selected based on these estimates.

Depending on the system design, the pilots can be several milliseconds apart. For example, in the IEEE 802.11n standard [8], a multiple access control (MAC) based training protocol is used for transmit and/or receive antenna selection. In it, a sequence of consecutive ‘training packets’ are transmitted to obtain the CSI of all antennas. The primary reason for doing this is to ensure that the physical layer protocols in the standard do not have to be modified considerably to accommodate AS training [15]. The pilots embedded in the physical layer header of each training packet help estimate the channel gains. Each training packet, which carries a physical layer header and a data payload, can be several milliseconds long. For this reason, the pilots sent across the training packets are also spaced several milliseconds apart. Thus, the CSI at the receiver is imperfect not just because of noise in the channel estimates but also because of training delays. Since different channels are estimated at different times, *the CSI at different antenna elements is outdated by different amounts* by the time data symbols are demodulated.

While receive AS has been explored extensively in the literature, most papers assume perfect CSI at the receiver. Imperfect CSI can lead to inaccurate selection and imperfect data decoding, both of which increase the symbol error probability (SEP) or the packet error rate (PER). Receive AS with imperfect channel estimates, but with only estimation errors due to noise, has been explored in [7], [16]–[20]. While [21], [22] considered outdated channel estimates, the unequal outdatedness of the CSI of the antennas was not factored in. While [23] considered unequal outdatedness, it selected the antenna with the highest estimated channel gain.

In this paper, we analyze and optimize the performance of AS over time-varying Rayleigh fading channels given a practical training model. We show that imperfect CSI has a significant impact on AS performance and argue that the selection criterion should account for the training delays (amount of outdatedness) encountered in any practical AS system.

V. Kristem is with Beceem Communications, Bangalore, India. He was with the Dept. of Electrical Communication Engineering (ECE) at the Indian Institute of Science (IISc), Bangalore, India during the course of this work. N. B. Mehta is with the ECE Dept. at IISc. A. F. Molisch is with the Dept. of Electrical Eng. at the University of Southern California, Los Angeles, CA, USA.

Emails: vinod.kristem@gmail.com, nbmehta@ece.iisc.ernet.in, andreas.molisch@ieee.org

A part of this paper has appeared in ICC 2009.

Intuitively, it should deemphasize in a monotonic fashion the more outdated estimates. Accordingly, we propose to use a selection criterion that weights the channel estimates to select the best antenna. We show that such a weighting is indeed optimal for minimizing SEP. We derive general closed-form expressions for the SEP of MPSK and MQAM constellations as a function of the selection weights and the antenna sounding pattern. We also characterize explicitly the optimal selection weights and study their asymptotic behavior. As we shall see, training delays coupled with noisy estimates lead to an error floor in the SEP, which does not occur when just noisy (or perfect) estimates are considered. Optimal selection weights lower the error floor significantly.

In addition to SEP, we also investigate the problem from a PER perspective, in which multiple symbols of the packet need to be received by the same antenna. Characterizing and minimizing the PER turns out to be a much harder problem analytically. We, therefore, develop an approximation for the PER and use it to determine the optimal weights. We also propose two new suboptimal selection algorithms for minimizing the PER that are computationally simple and effective. For coded packets, the benefits of weighted selection are verified using the practical channel mother code specified in third generation 3GPP cellular system standard.

The paper is organized as follows. The system model is developed in Sec. II. Symbol error probability with weighted selection is analyzed and optimized in Sec. III. Packet error probability is dealt with in Sec. IV. The results and conclusions follow in Sec. V and Sec. VI, respectively. Several mathematical derivations and proofs are relegated to the Appendix.

II. MODEL

Consider a system with one transmit antenna, N receive antennas, and one RF chain at the receiver. Let $h_k(t)$ denote the frequency-flat channel between the transmitter and the k^{th} receive antenna at time t . It is modeled as a circularly symmetric complex Gaussian random variable (RV) with unit variance. Furthermore, the channel gains for different receive antennas are assumed to be independent and identically distributed (i. i. d.), which is the case when the receive antennas are spaced sufficiently apart [24].

A. Channel Estimation

We consider a transmission format in which multiple pilot symbols precede multiple data symbols, as shown in Fig. 1. The transmitter sends a pilot symbol p_p (of duration T_s) to each receive antenna sequentially so that all N channels can be estimated and the optimum antenna selected to receive the data symbols block.¹ The k^{th} receive antenna is estimated at time T_k . Two consecutive pilot symbols are separated in time by a duration T_p . Note that the order in which antennas are

¹In order to reduce overhead IEEE 802.11n usually transmits payload data together with each pilot tone. These payload data *have* to be received with the same antenna element for which the pilot tone is intended. Thus, the error probability for the payload does not depend on any selection algorithm, and is irrelevant for the purposes of this paper. Note that T_p also captures the inter-packet spacing required to switch between antennas. However, the switching time is small compared to a packet duration. It will be verified in Sec. V.

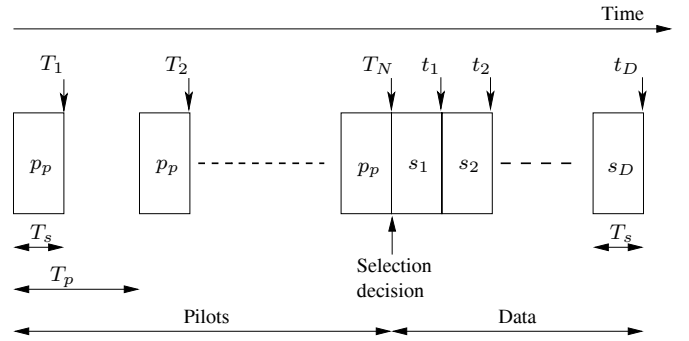


Fig. 1. Training for receive antenna selection

trained does not affect the SEP (or PER) since the channel gains of different antennas are assumed to be i. i. d.

Pilot-based channel estimation is imperfect due to:

1. *Noise-induced channel estimation errors*: The signal received by the k^{th} antenna is

$$r_k(T_k) = p_p h_k(T_k) + n_k(T_k),$$

where p_p is a complex pilot symbol with $|p_p|^2 = E_p$, and $n_k(t)$ is a circularly symmetric complex Gaussian process with zero mean and power N_0 that is independent of $h_k(t)$. Therefore, the channel estimate for the k^{th} receive antenna is

$$\hat{h}_k(T_k) = \frac{p_p^* r_k(T_k)}{|p_p|^2} = h_k(T_k) + e_k, \quad (1)$$

where the noise-induced channel estimation error $e_k = \frac{n_k(T_k)}{p_p}$ has a variance $\sigma_e^2 = \frac{N_0}{E_p}$. Here, E_p is the pilot symbol energy.

2. *Outdated channel estimates*: Due to the time-varying nature of the wireless links, the N channels will have changed by the time data transmission starts. Using a first order autoregressive model, the channel for receive antenna k at time $t + \delta$ can be written in terms of the channel at time t as [21], [25]

$$h_k(t + \delta) = \rho_k(\delta) h_k(t) + \sqrt{1 - |\rho_k(\delta)|^2} n'_k(t + \delta), \quad (2)$$

where $\rho_k(\delta)$ is the channel correlation coefficient.² The variation $n'_k(t + \delta)$, $k = 1, 2, \dots, N$, is a circularly symmetric complex Gaussian RV with unit variance that is independent of $h_k(t)$. The channel correlation coefficient depends on the time difference δ and the Doppler spectrum (which, in turn, depends on the velocity, angular spectrum, and antenna pattern of the mobile station [24]). Our derivations in Sec. III and Sec. IV are valid for arbitrary Doppler spectra; for the simulations in Sec. V, we use the classical Jakes spectrum [24] in which $\rho_k(\delta) = J_0(2\pi f_d \delta)$, where $J_0(\cdot)$ is the zeroth order Bessel function of the first kind [26] and f_d is the maximum Doppler frequency.

²The regressive model in (2) uses the simplifying assumption that the channel realizations at different times can be computed based only on the correlation with the channel at time $t = 0$, and not as a realization of a stochastic process with a continuous correlation function. The approximation is good so long as the maximum Doppler frequency times δ is small.

B. Weighted Antenna Selection

The standard selection criterion is to pick the antenna with the highest (estimated) channel gain [16]. However, as we shall see, this is not optimal when the CSI of different antennas is outdated by different amounts – it is possible that the antenna with the highest channel gain could have severely outdated CSI and should not be selected. For the data symbol transmitted at time t_i , we propose selecting the antenna based on *weighted* channel gain estimates as follows:

$$[\hat{1}]_i = \underset{1 \leq k \leq N}{\operatorname{argmax}} w_{k,i} \left| \hat{h}_k \right|^2. \quad (3)$$

The symbol $[\hat{1}]_i$, following standard order-statistics notation, denotes the index of the selected antenna, with the cap ($[\cdot]$) showing that the selection decision was based on estimates. Antenna $[\hat{1}]_i$ is then used for receiving the data symbol. We will see that, because of time-varying nature of the channel, the optimal weights – and, hence, the selected antenna – depend on i . We will show later that linear weighting is indeed the optimal strategy for minimizing the SEP.

C. Data Reception

As shown in Fig. 1, the pilots are followed by D data symbols, each of duration T_s and energy E_s ; we assume that the duration of a data symbol is much shorter than the coherence time of the channel. When the data symbol s_i is transmitted at time t_i , the signal received by antenna $[\hat{1}]_i$ is given by³

$$y_{[\hat{1}]_i}(t_i) = h_{[\hat{1}]_i}(t_i)s_i + n_{[\hat{1}]_i}(t_i). \quad (4)$$

The data symbols are equi-probable and derived from the MPSK or MQAM constellations. For MPSK, $s_i \in \{\sqrt{E_s} \exp(j\frac{2\pi m}{M}), m = 0, \dots, M-1\}$. For MQAM, $s_i = \sqrt{\frac{3E_s}{2(M-1)}}(a_I + ja_Q)$, where $a_I, a_Q \in \{2l-1-\sqrt{M}, l = 1, \dots, \sqrt{M}\}$.

III. SYMBOL ERROR PROBABILITY ANALYSIS AND OPTIMIZATION

We now analyze the SEP for the i^{th} symbol for receive AS with imperfect and outdated CSI for both MPSK and MQAM. Henceforth, we simplify our notation as follows: we denote $\hat{h}_k(T_k)$ by \hat{h}_k , $n'_k(t)$ by n'_k , $\rho_k(t_i - T_k)$ by $\rho_k^{(i)}$, and $n_k(t)$ by n_k . $\Pr(A)$, $\mathbf{E}[A]$, and $\mathbf{var}[A]$ shall denote the probability, expectation, and variance of A , respectively. Similarly, $\Pr(A|B)$, $\mathbf{E}[A|B]$, and $\mathbf{var}[A|B]$ shall denote the conditional probability, expectation, and variance of A given B , respectively. x^* shall denote the complex conjugate of x .

The imperfect channel estimates are used for both selection and data decoding. Therefore, the maximum likelihood (ML) decision variable, \mathcal{D} , for the signal received by antenna $[\hat{1}]_i$ is:

$$\mathcal{D} = \hat{h}_{[\hat{1}]_i}^* y_{[\hat{1}]_i}(t_i).$$

Using (1) and (2), we can write the channel at time t_i in terms of its estimate. Hence,

$$\mathcal{D} = \hat{h}_{[\hat{1}]_i}^* \left(\rho_{[\hat{1}]_i}^{(i)} (\hat{h}_{[\hat{1}]_i} - e_{[\hat{1}]_i}) s_i + \sqrt{1 - |\rho_{[\hat{1}]_i}^{(i)}|^2} n'_{[\hat{1}]_i} s_i + n_{[\hat{1}]_i} \right). \quad (5)$$

The above equation brings out one important aspect associated with training for antenna selection in time-varying fading channels. It can be seen that the decision variables for symbols transmitted at different times will be different, and so will their error probabilities. This is quantified by the following Lemma about the statistics of \mathcal{D} , which turn out to depend on i .

Lemma 1: Conditioned on $\{\hat{h}_k\}_{k=1}^N$ and s_i , \mathcal{D} is a complex Gaussian RV with conditional mean and variance given by

$$\mu_{\mathcal{D}} \triangleq \mathbf{E}[\mathcal{D} | \{\hat{h}_k\}_{k=1}^N, s_i] = \left| \hat{h}_{[\hat{1}]_i} \right|^2 \rho_{[\hat{1}]_i}^{(i)} s_i q^2, \quad (6)$$

$$\sigma_{\mathcal{D}}^2 \triangleq \mathbf{var}[\mathcal{D} | \{\hat{h}_k\}_{k=1}^N, s_i] = \left(1 - |\rho_{[\hat{1}]_i}^{(i)}|^2\right) |s_i|^2 \left| \hat{h}_{[\hat{1}]_i} \right|^2 + \left| \hat{h}_{[\hat{1}]_i} \right|^2 \left| \rho_{[\hat{1}]_i}^{(i)} \right|^2 |s_i|^2 \sigma_e^2 q^2 + \left| \hat{h}_{[\hat{1}]_i} \right|^2 N_0, \quad (7)$$

where $q^2 \triangleq 1/(1 + \sigma_e^2)$.

Proof: The proof is given in Appendix A. ■

We are now ready to derive the SEPs for MPSK and MQAM in the following two theorems. Let $\gamma \triangleq \frac{E_s}{N_0}$ (average SNR per branch) and $\varepsilon \triangleq \frac{E_p}{E_s}$.

Theorem 1: With training delays and noisy channel estimates, the SEP for the i^{th} MPSK symbol received at time t_i when the selection weight for antenna k is w_k is

$$P_i^{\text{MPSK}}(\gamma) = \frac{1}{\pi} \sum_{m=1}^N \sum_{r=0}^{N-1} \sum_{\substack{l_0, \dots, l_r=1 \\ l_0=1, l_1 \neq \dots \neq l_r \neq m}}^N \frac{(-1)^r}{r! \left(1 + \sum_{j=1}^r \frac{w_m}{w_{l_j}}\right)} \left[\frac{M-1}{M} \pi - \tan^{-1} \left(\frac{\sqrt{\alpha_m^{(i)}(\gamma, w_{l_1}, \dots, w_{l_r})} \tan\left(\frac{M-1}{M} \pi\right)}{\sqrt{\alpha_m^{(i)}(\gamma, w_{l_1}, \dots, w_{l_r})}} \right) \right], \quad (8)$$

where

$$\alpha_m^{(i)}(\gamma, w_{l_1}, \dots, w_{l_r}) \triangleq 1 + \frac{\left(1 + \sum_{j=1}^r \frac{w_m}{w_{l_j}}\right)}{\varepsilon \left| \rho_m^{(i)} \right|^2 \sin^2\left(\frac{\pi}{M}\right)} \left(\varepsilon \left(1 - \left| \rho_m^{(i)} \right|^2\right) + \frac{1+\varepsilon}{\gamma} + \frac{1}{\gamma^2} \right). \quad (9)$$

Proof: The proof is relegated to Appendix B. ■

The symbol $\sum_{l_0=1}^N \sum_{\substack{l_1, \dots, l_r=1 \\ l_1 \neq \dots \neq l_r \neq m}}^N$ above denotes $\sum_{l_0=1}^1 \sum_{\substack{l_1=1 \\ (l_1 \neq m)}}^N \sum_{\substack{l_2=1 \\ (l_2 \neq m, l_2 \neq l_1)}}^N \dots \sum_{\substack{l_r=1 \\ (l_r \neq m, l_r \neq l_1, \dots, l_r \neq l_{r-1})}}^N$. This is done to keep the notation compact.

Theorem 2: With training delays and noisy channel estimates, the SEP for the i^{th} MQAM symbol received at time t_i is given by

³For brevity, we shall refer to the data symbol transmitted at time t_i as the i^{th} data symbol.

$$\begin{aligned}
P_i^{\text{MQAM}}(\gamma) &= 2 \left(1 - \frac{1}{\sqrt{M}}\right) \sum_{m=1}^N \sum_{r=0}^{N-1} \sum_{\substack{l_0, \dots, l_r=1 \\ l_0, \dots, l_r \neq m}}^N \frac{(-1)^r / r!}{1 + \sum_{j=1}^r \frac{w_m}{w_{l_j}}} \\
&\quad \times \left(1 - \frac{1}{\sqrt{\beta_m^{(i)}(\gamma, w_{l_1}, \dots, w_{l_r})}}\right) \\
&\quad - \sum_{m=1}^N \sum_{r=0}^{N-1} \sum_{\substack{l_0, \dots, l_r=1 \\ l_0, \dots, l_r \neq m}}^N \frac{(-1)^r / r!}{1 + \sum_{j=1}^r \frac{w_m}{w_{l_j}}} \\
&\times \left(1 - \frac{1}{\sqrt{M}}\right)^2 \left(1 - \frac{4 \tan^{-1} \left(\sqrt{\beta_m^{(i)}(\gamma, w_{l_1}, \dots, w_{l_r})} \right)}{\pi \sqrt{\beta_m^{(i)}(\gamma, w_{l_1}, \dots, w_{l_r})}}\right), \quad (10)
\end{aligned}$$

where

$$\begin{aligned}
&\beta_m^{(i)}(\gamma, w_{l_1}, \dots, w_{l_r}) \\
&\triangleq 1 + \frac{\left(1 + \sum_{j=1}^r \frac{w_m}{w_{l_j}}\right)}{\varepsilon \left|\rho_m^{(i)}\right|^2 \left(\frac{3}{2(M-1)}\right)} \left(\varepsilon \left(1 - \left|\rho_m^{(i)}\right|^2\right) + \frac{1+\varepsilon}{\gamma} + \frac{1}{\gamma^2}\right). \quad (11)
\end{aligned}$$

Proof: The proof is given in Appendix C. ■

A. Optimal Selection Weights

With the above general formulae in place, we are now ready to derive the optimal selection weights $\left\{w_{k,i}^{\text{opt}}\right\}_{k=1}^N$ that minimize the SEP for the i^{th} MPSK or MQAM symbol at an average SNR γ .

Theorem 3: For $1 \leq k \leq N$, the optimal selection weights that minimize the SEP of the i^{th} MPSK or MQAM symbol received at time t_i are given by

$$w_{k,i}^{\text{opt}}(\gamma) = \frac{\left|\rho_k^{(i)}\right|^2}{\left(\varepsilon \left(1 - \left|\rho_k^{(i)}\right|^2\right) + \frac{1+\varepsilon}{\gamma} + \frac{1}{\gamma^2}\right)}. \quad (12)$$

Furthermore, linearly weighting the channel estimates as done in (3) is the optimal strategy.

Proof: The proof is given in the Appendix D. ■

Observe that the optimal selection rule requires the knowledge of the temporal channel correlation coefficients and the pilot and data SNRs. Knowing the data SNR is equivalent to knowing the pilot SNR because the ‘pilot power boosting’ factor, ε , is always known a priori at the receiver. Notice that even the conventional coherent receiver that uses the unweighted selection rule requires knowledge of the pilot and data SNRs. Thus, the only additional information needed in a coherent receiver that uses the optimal weights is the temporal channel correlation. The temporal correlation can be estimated from the noisy estimates of the channel gains because it depends on array geometry, antenna radiation pattern, and the scattering environment, and, thus, changes on a much slower time scale than the instantaneous fading. Several techniques

have been developed for this purpose, see, for example, [27], [28] and the references therein.

The optimal weights can take any value from 0 to infinity. Notice that the optimal weight for an antenna k increases as its channel correlation coefficient increases, which is in line with our intuition. In typical regimes of operation of $f_d T_p$, the correlation coefficient decreases as the training delay increases. Thus, as expected, the optimal weight for an antenna also monotonically decreases as the training delay increases. The result above also implies that the optimal selection weights – and, hence, the selected antenna – can be different for data symbols transmitted at different times. This will play an important role in understanding the suboptimal algorithm proposed later for PER minimization.

When the training delays are the same, i.e., $\rho_k^{(i)} = \rho$, the optimum weights do not depend on k and i , which is equivalent to setting all the weights to unity, i.e., performing selection without weighting. For large training delays ($\left|\rho_k^{(i)}\right| \ll 1$) the optimum weights, after removing common factors, simplify to the following ρ -weighting scheme:

$$w_{k,i}^{\text{opt}}(\gamma) \approx \left|\rho_k^{(i)}\right|^2. \quad (13)$$

Interestingly, using MMSE channel prediction to handle the time-variations also leads to the ρ -weighting scheme. Thus, Theorem 3 also shows that the MMSE prediction is not SEP optimal.

B. Asymptotic Behavior of SEP with Optimal Weights

We now consider the asymptotic behavior of the SEP expressions in (8) and (10) as the average SNR per branch, γ , increases. For MPSK, let $\lim_{\gamma \rightarrow \infty} \alpha_k^{(i)}(\gamma, w_{l_1}, \dots, w_{l_r}) \triangleq \alpha_{k,\text{asm}}^{(i)}(w_{l_1}, \dots, w_{l_r})$ and $P_{i,\text{asm}}^{\text{MPSK}} \triangleq \lim_{\gamma \rightarrow \infty} P_i^{\text{MPSK}}(\gamma)$. For MQAM, let $\lim_{\gamma \rightarrow \infty} \beta_k^{(i)}(\gamma, w_{l_1}, \dots, w_{l_r}) \triangleq \beta_{k,\text{asm}}^{(i)}(w_{l_1}, \dots, w_{l_r})$ and $P_{i,\text{asm}}^{\text{MQAM}} \triangleq \lim_{\gamma \rightarrow \infty} P_i^{\text{MQAM}}(\gamma)$. When training delays are absent, $\rho_k^{(i)} = 1$, for all k and i . From (9) and (11), it follows that $\alpha_{k,\text{asm}}^{(i)}(\cdot) = 1$ and $\beta_{k,\text{asm}}^{(i)}(\cdot) = 1$, for all k and i for the optimal weights. Substituting these asymptotic values in (8) and (10), we can show that $P_{i,\text{asm}}^{\text{MPSK}} \equiv 0$ and $P_{i,\text{asm}}^{\text{MQAM}} \equiv 0$, which is consistent with the results in [16].

For non-zero training delays, we have $\rho_k^{(i)} < 1$. From (12), we can see that the asymptotic optimal weights (after removing common factors) equal

$$\lim_{\gamma \rightarrow \infty} w_{k,i}^{\text{opt}}(\gamma) = \frac{\left|\rho_k^{(i)}\right|^2}{1 - \left|\rho_k^{(i)}\right|^2}. \quad (14)$$

Substituting the above weights in (9) and (11) and simplifying further we get

$$\alpha_{k,\text{asm}}^{(i)}(\cdot) = 1 - \csc^2\left(\frac{\pi}{M}\right) \left(r + 1 - \frac{1}{\left|\rho_k^{(i)}\right|^2} - \sum_{j=1}^r \frac{1}{\left|\rho_{l_j}^{(i)}\right|^2}\right),$$

$$\beta_{k,\text{asm}}^{(i)}(\cdot) = 1 - \frac{2(M-1)}{3} \left(r + 1 - \frac{1}{|\rho_k^{(i)}|^2} - \sum_{j=1}^r \frac{1}{|\rho_{l_j}^{(i)}|^2} \right).$$

Upon substituting these asymptotic values in the SEP formulae for MPSK and MQAM, we find that $P_{i,\text{asm}}^{\text{MPSK}}$ and $P_{i,\text{asm}}^{\text{MQAM}}$ are no longer identically 0. Hence, an irreducible error floor exists at high SNR, and depends on the correlations $\{\rho_k^{(i)}\}_{k=1}^N$.

IV. SELECTION TO MINIMIZE PACKET ERROR RATE (PER)

In practice, non-zero switching times are required to switch between antennas. Unless these switching times are much smaller than the data symbol duration, they motivate the practical restriction that all the data symbols of a packet must be received by the same antenna. This constraint introduces a new twist to the selection problem since different symbols of a packet experience different training delays. The fading-averaged packet error rate (PER) cannot be directly determined from the fading-averaged SEPs of the D different symbols since the same antenna and antenna estimate is used to decode the all data symbols in the packet. As we shall see below, this makes an exact analysis significantly more difficult.

We first analyze the case where an uncoded packet is transmitted, and show that an approximation for the PER can still be derived and used to determine the optimal selection weights. Since the analysis of receive AS for the coded packet case remains an intractable problem, we use simulations in the next section to study weighted selection for coded packet transmissions. The weighted selection criteria motivated by and validated for the uncoded packet case considered below shall prove useful for the coded case.

A. Exact PER Analysis

An uncoded packet is in error when at least one of the D data symbols is decoded incorrectly. We use the weighted selection rule given in (3) except that the weights, w_k , and the selected antenna, $[\hat{1}]$, do not depend on the symbol index i since all the D data symbols are now received by same antenna. Conditioned on $\{\hat{h}_k\}_{k=1}^N$, the symbol errors are independent. Therefore, for MPSK, the PER conditioned on the channel gains equals

$$\begin{aligned} \text{PER} \left(\gamma | \{\hat{h}_k\}_{k=1}^N \right) &= 1 - \prod_{i=1}^D \left(1 - \frac{1}{\pi} \int_{\theta_i=0}^{\frac{M-1}{M}\pi} \exp \left(- \frac{|\hat{h}_{[\hat{1}]}|^2 b_{[\hat{1}]}^{(i)}}{\sin^2 \theta_i} \right) d\theta_i \right), \\ &= \sum_{i=1}^D \sum_{\substack{q_1, \dots, q_i=1 \\ q_1 \neq q_2 \dots \neq q_i}}^D \frac{(-1)^{i+1}}{i! \pi^i} \\ &\times \int_{\theta_{q_1}=0}^{\frac{M-1}{M}\pi} \dots \int_{\theta_{q_i}=0}^{\frac{M-1}{M}\pi} \exp \left(- |\hat{h}_{[\hat{1}]}|^2 \sum_{l=1}^i \frac{b_{[\hat{1}]}^{(q_l)}}{\sin^2 \theta_{q_l}} \right) d\theta_{q_1} \dots d\theta_{q_i}. \end{aligned} \quad (15)$$

Along lines similar to Theorem 1, we can now compute the fading-averaged PER and get

$$\begin{aligned} \text{PER}(\gamma) &= \sum_{i=1}^D \sum_{k=1}^N \sum_{r=0}^{N-1} \sum_{\substack{l_0, \dots, l_r=1 \\ l_0=1, l_1 \neq \dots \neq l_r \neq k}}^N \sum_{\substack{q_1, \dots, q_i=1 \\ q_1 \neq q_2 \dots \neq q_i}}^D \frac{(-1)^{r+i+1}}{r! i! \pi^i (1 + \sigma_e^2)} \\ &\times \int_{\theta_{q_1}=0}^{\frac{M-1}{M}\pi} \dots \int_{\theta_{q_i}=0}^{\frac{M-1}{M}\pi} \left(\sum_{l=1}^i \frac{b_k^{(q_l)}}{\sin^2 \theta_{q_l}} + \frac{1 + \sum_{j=1}^r \frac{w_k}{w_{l_j}}}{1 + \sigma_e^2} \right)^{-1} d\theta_{q_1} \dots d\theta_{q_i}. \end{aligned} \quad (16)$$

This can be reduced to an $(i-1)$ -dimensional integral using (29). However, any further simplification of PER is not possible. The same problem also arises for MQAM packets.

Consequently, finding the optimal weights for minimizing the PER is a non-trivial problem. We present below three different approaches that overcome this barrier. Surprisingly, all lead to a similar improved performance. In the first approach, we derive a tractable and closed-form approximate expression for the PER that involves no integrals whatsoever. Therefore, computationally efficient gradient search algorithms can now be employed to find the optimal weights that minimize the PER. In the other two approaches, we propose sub-optimal selection algorithms that use the SEP optimality results from the previous section.

B. PER Approximation

The key step that enables the approximation is captured in the Lemma below, which provides a bound on the integrand in (16).

Lemma 2: If $\{a_k\}_{k=1}^n$ and b are non-negative numbers, then

$$\int_{\theta_n=0}^{\frac{M-1}{M}\pi} \dots \int_{\theta_1=0}^{\frac{M-1}{M}\pi} \left(\sum_{k=1}^n \frac{a_k}{\sin^2 \theta_k} + b \right)^{-1} d\theta_1 \dots d\theta_n \geq \frac{1}{b} \prod_{k=1}^n \tau_k, \quad (17)$$

where

$$\begin{aligned} \tau_k &\triangleq \frac{M-1}{M} \pi - \sqrt{\frac{a_k}{\sum_{i=k}^n a_i + b}} \\ &\times \tan^{-1} \left(\sqrt{\frac{\sum_{i=k}^n a_i + b}{a_k}} \tan \left(\frac{M-1}{M} \pi \right) \right). \end{aligned} \quad (18)$$

Proof: The proof is given in Appendix E. ■

Using the above Lemma, it can be shown that the integral term in (16) is lower bounded as:

$$\begin{aligned} \int_{\theta_{q_1}=0}^{\frac{M-1}{M}\pi} \dots \int_{\theta_{q_i}=0}^{\frac{M-1}{M}\pi} \left(\sum_{l=1}^i \frac{b_k^{(q_l)}}{\sin^2 \theta_{q_l}} + \frac{1 + \sum_{j=1}^r \frac{w_k}{w_{l_j}}}{1 + \sigma_e^2} \right)^{-1} d\theta_{q_1} \dots d\theta_{q_i} \\ \geq \left(\prod_{m=1}^i z_{r,i,k}^{(m)} \right) \frac{(1 + \sigma_e^2)}{\left(1 + \sum_{j=1}^r \frac{w_k}{w_{l_j}} \right)}, \end{aligned}$$

where $z_{r,i,k}^{(m)} = \frac{M-1}{M} \pi - \frac{1}{\sqrt{g_{r,i,k}^{(m)}}} \tan^{-1} \left(\sqrt{g_{r,i,k}^{(m)}} \tan \left(\frac{M-1}{M} \pi \right) \right)$ and $g_{r,i,k}^{(m)} \triangleq \frac{\sum_{l=m}^i b_k^{(q_l)}}{b_k^{(q_m)}} + \frac{1 + \sum_{j=1}^r \frac{w_k}{w_{l_j}}}{b_k^{(q_m)} (1 + \sigma_e^2)}$.

Substituting this bound in the various terms of the PER equation and simplifying leads to the following approximation:

$$\text{PER}(\gamma) \approx \sum_{i=1}^D \sum_{k=1}^N \sum_{r=0}^{N-1} \frac{(-1)^{r+i+1}}{r!i!\pi^i} \left(\prod_{m=1}^i z_{r,i,k}^{(m)} \right) \\ \times \sum_{\substack{l_0, \dots, l_r=1 \\ l_0=1, l_1 \neq \dots \neq l_r \neq k}}^N \sum_{\substack{q_1, \dots, q_i=1 \\ q_1 \neq q_2 \dots \neq q_i}}^D \frac{1}{\left(1 + \sum_{j=1}^r \frac{w_k}{w_{i_j}}\right)}. \quad (19)$$

Note that this is an approximation and not a bound because of the alternating signs of various terms. Computationally efficient gradient search algorithms, such as the Nelder-Mead method implemented in Matlab, can now be employed to find the optimal selection weights. By normalizing one of the weights to unity, the gradient search algorithms effectively need to search over an $N - 1$ dimensional space of positive real numbers. Notice that even this provides a significant computational advantage over a Monte Carlo based search that first measures the PER and then iterates over different weights.

Despite fast gradient search techniques being available, this is computationally intensive for larger N . This motivates us to propose and investigate the performance of the following two sub-optimal approaches to find the selection weights.

C. Approach 2: Select Antenna That is SEP Optimal Most Often

Consider an ideal receiver in which the antennas can be switched on a symbol-by-symbol basis. In this case, the PER is minimized by using for each symbol index its SEP optimal antenna. This involves evaluating for each symbol index its optimal selection weights and then selecting the best antenna as per (3) and (12). It is indeed possible that the selected antennas are different for different data symbol transmission indices since the corresponding optimal weights are different.

The above procedure suggests the following algorithm for selecting the best antenna when the same antenna must be used for receiving the entire packet: *Use the antenna that is SEP optimal for the most time in a packet.* Mathematically, the rule can be stated as:

$$[\hat{1}] = \underset{1 \leq k \leq N}{\operatorname{argmax}} \sum_{i=1}^D I_{\{[\hat{1}]_i = k\}}, \quad (20)$$

where $[\hat{1}]_i$ is given by equation (3) and $I_{\{x\}}$ is the indicator function that equals 1 if x is true, and is 0 otherwise. Since we have derived a closed-form expression for the SEP optimal weights, this algorithm is fast. It requires only $O(DN)$ calculations and is guaranteed to terminate.

D. Approach 3: Select Antenna With Maximum Post-Processing SNR

From the expression for SEP optimal weights, we can see that the optimal selection rule also maximizes the post-processing SNR. This is because the post-processing SNR, $\Gamma_k^{(i)}$, when the i^{th} MPSK data symbol is received by k^{th} antenna, can be shown to be directly proportional to $|\hat{h}_k|^2 w_{k,i}^{\text{opt}}$.

This suggests the following algorithm for selecting the antenna: *Calculate the post-processing SNR for each of the data symbols in the packet and use the antenna that maximizes the total post-processing SNR over the packet, i.e.,*

$$[\hat{1}] = \underset{1 \leq k \leq N}{\operatorname{argmax}} \left(\sum_{i=1}^D w_{k,i}^{\text{opt}} \right) |\hat{h}_k|^2. \quad (21)$$

V. SIMULATIONS

We now present graphically the results derived in Sections III and IV, and study the effect of parameters such as N , $f_d T_p$, and $\{w_k\}_{k=1}^N$ on the SEP and PER. We also compare these with Monte Carlo simulations with 10^4 samples generated for each SNR ($\gamma \triangleq E_s/N_0$). The simulator of [29] is used to generate the time-varying Rayleigh channels. From Sec. II-A, the correlation values for $k = 1, 2, \dots, N$ and $i = 1, 2, \dots, D$ equal $\rho_k^{(i)} = J_0(2\pi f_d((N-k)T_p + iT_s))$. Throughout the simulations the pilot SNR is kept the same as data SNR ($\varepsilon = 1$). Unless mentioned otherwise, the SEP of the first data symbol ($i = 1$) is plotted. We first study SEP and then PER.

Figures 2 and 3 plot the SEP as a function of the SNR for MPSK and MQAM, respectively, for $N = 4$ antennas. One can see that the SEP always decreases to 0 as the SNR increases when $f_d T_p = 0$, even with noisy estimates. On the other hand, an error floor exists when $f_d T_p > 0$, which increases as $f_d T_p$ increases. Also shown is the effect of different selection weights on the SEP. For $f_d T_p \approx 0$, all the six curves for the different weighting schemes coincide because $w_{k,i}^{\text{opt}} \approx 1$. For large $f_d T_p$, $w_{k,i}^{\text{opt}}(\gamma) = |\rho_k|^2$ performs almost as well as optimal weighting, which is in line with the analysis in Sec. III-A. We no longer plot the simulations given the excellent match between analytical and simulation results for all the weighting schemes.⁴ Similar behavior is observed for higher values of i . As i increases, the relative gains obtained by using the optimal selection weights decrease. This is because the relative variation among the weights of different antennas decreases as all the weights decrease towards 0. The effect of T_p/T_s is studied in Fig. 4. It shows that optimal weighting improves performance in both low and high Doppler regimes.

Figure 5 shows how often each antenna is selected by optimal weighting for different values of the normalized Doppler spread. At an SNR of 12 dB and $f_d T_p = 0.06$, antenna 1 ($\rho_1^{(1)} = 0.6866$) and antenna 4 ($\rho_4^{(1)} = 0.9996$) get selected 1.4% and 58.8% of the time, respectively, for decoding the first data symbol. However, for $f_d T_p = 0.01$, the numbers change to 21.7% and 27.2% for antenna 1 ($\rho_1^{(1)} = 0.9905$) and antenna 4 ($\rho_4^{(1)} = 0.9999$), respectively.

Figure 6 compares the SEP of MPSK for $N = 2, 4$, and 8 receive antennas as a function of the SNR at $f_d T_p = 0.01$ for the no-weighting and optimal weighting selection schemes. In the no-weighting scheme, increasing the number of receive antennas worsens performance. This is because selection becomes more inaccurate – and unequally so for different

⁴For MQAM, there is a small mismatch between analytical and simulation results in Fig. 3. This is explained in Appendix C, which derives the SEP for MQAM.

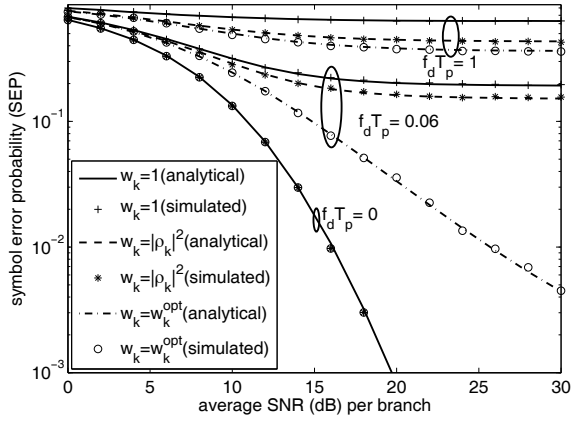


Fig. 2. Effect of normalized Doppler spread and weights (8PSK, $T_p = 10T_s$, and $N = 4$).

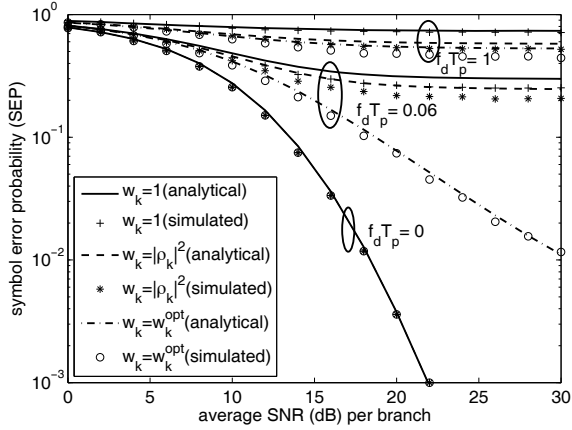


Fig. 3. Effect of normalized Doppler spread and weights (16QAM, $T_p = 10T_s$, and $N = 4$).

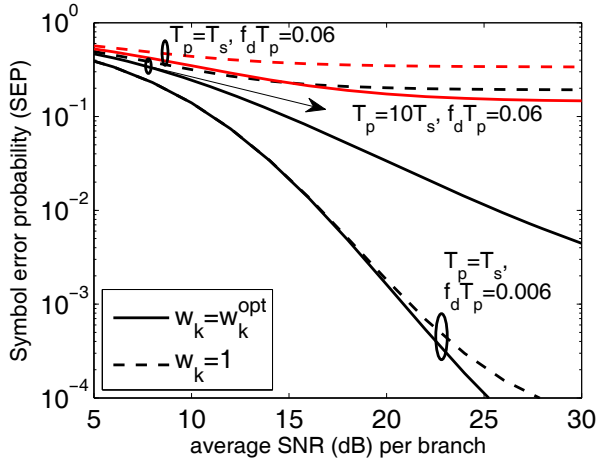


Fig. 4. Effect of normalized Doppler spread and the ratio T_p/T_s (8PSK and $N = 4$).

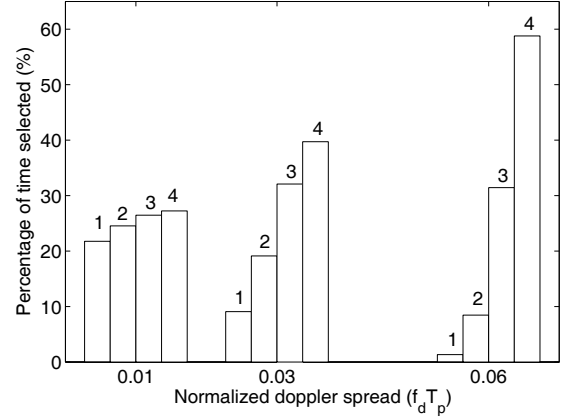


Fig. 5. Percentage of time with which different antennas are selected for data reception as a function of $f_d T_p$ (8PSK, $T_p = 10T_s$, and $N = 4$). Pilots are sent by the transmit antennas 1, 2, 3, and 4 in sequence.

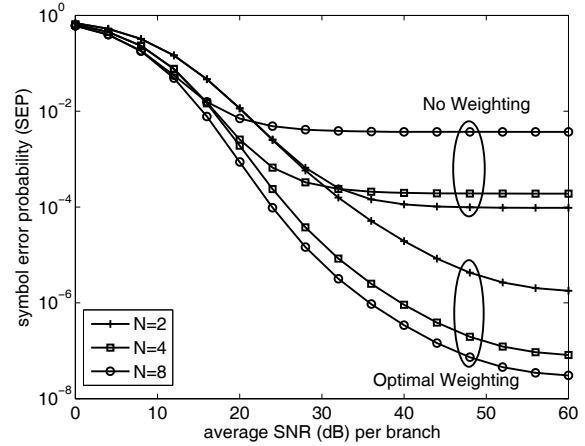


Fig. 6. Effect of number of receive antennas and weights for fixed Doppler spread and T_p (8PSK, $T_p = 10T_s$, and $f_d T_p = 0.01$).

antennas – as the training delays increase. However, the optimal weights, which account for this, remedy this problem. Furthermore, they also substantially reduce the error floors by one to two orders of magnitude.

An alternative view is presented in Fig. 7, which compares the SEP of MPSK for $N = 2, 4$, and 8 antennas at an SNR of 10 dB as a function of the Doppler spread. For no-weighting, $N = 8$ outperforms others when $0 \leq f_d T_p \leq 0.017$. However, for $0.017 \leq f_d T_p \leq 0.044$ and $f_d T_p \geq 0.044$, $N = 4$ and $N = 2$, respectively, are the best choices. In contrast, for optimal weighting, $N = 8$ is always best choice.⁵ However, for higher Doppler spreads, the performance difference between smaller and larger number of antennas decreases.

The effect of different training delays for different antennas is studied in Fig. 8. Also plotted is the SEP for the hypothetical case where the training delays are the same and lead to a worst case correlation of $\rho_k = \rho_{\min}$ (maximum training delay) or a

⁵Note that the conclusions would be different if one assumed a fixed overall energy budget, so that using more pilot tones reduces the available energy for the payload data. In that case, more antennas need not be better even with weighted selection.

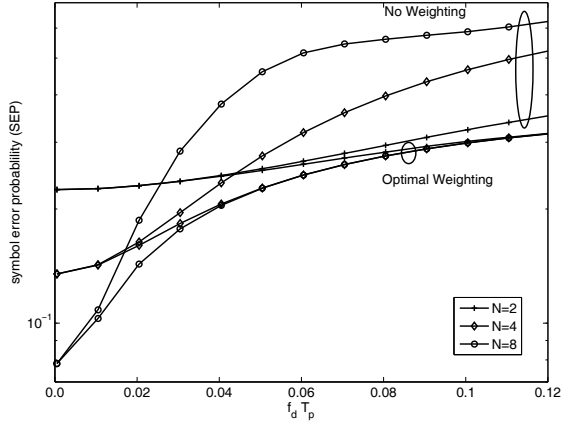


Fig. 7. Effect of number of receive antennas, Doppler spread, and weights for fixed T_p (8PSK, $T_p = 1\text{ms}$, $T_p = 10T_s$, and 10 dB SNR).

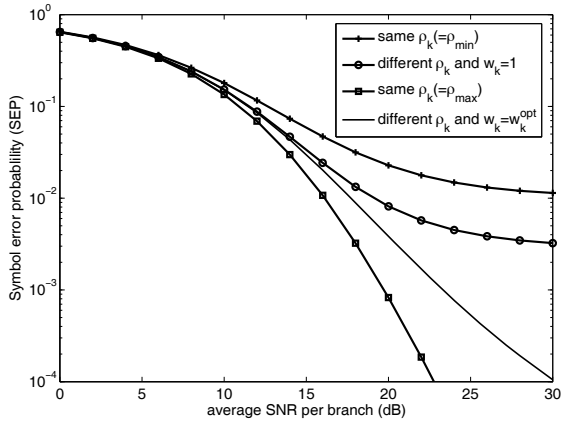


Fig. 8. Effect of different training delays for different antennas (8PSK, $f_d T_p = 0.016$, $T_p = 10T_s$, and $N = 4$).

best case correlation of $\rho_k = \rho_{max}$ (minimum training delay). It can be seen that the difference in training delays among the antennas has a greater impact at higher SNR values.

Next, we consider weighted antenna selection for packet reception. Figure 9 plots the PER from simulations when the receive antenna is selected: (i) without using any weights, (ii) using the weights obtained from the PER approximation (Sec. IV-B), and (iii) using the most often SEP optimal antenna (Sec. IV-C). Selection based on the total post-processing SNR (Sec. IV-D) is not shown as it is very close to that of the above two algorithms. We see that weighted selection significantly improves the PER compared to no weighting. Furthermore, the different selection weighting approaches result in similar performance. This is because, with high probability, the antenna that maximizes the post-processing SNR will remain SEP-optimal for many data symbols in the packet. If the channel changes significantly between adjacent data symbols, *i.e.*, at high Doppler, Approach 2 performs marginally better than Approach 3. While the PER approximation turns out to be about 3 dB loose in approximating the PER, it is still a good tool for selecting the receive antenna. To benchmark the

proposed suboptimal algorithms, the figure also plots the PER if a genie could somehow tell the receiver which antenna is optimal.⁶

Finally, in Fig. 10 we study weighted selection in a practical coded system. For this, we used the rate 1/3 mother convolutional code specified in the 3GPP Wideband CDMA standard [30]. Its generator polynomial is $G = [133\ 171\ 165]$. Hard decision Viterbi decoding was performed at the receiver. Each codeword/packet is 100 bits long and is 8PSK modulated. Bit error rate (BER) is plotted to enable a direct comparison with the uncoded results, for which the SEP was shown. The antenna is selected using suboptimal criteria proposed in Sections IV-C and IV-D. The BER obtained by choosing the genie-aided optimal antenna is also plotted as a benchmark. The observations are similar to the uncoded PER case. Weighted selection again outperforms no-weighting. Furthermore, the performance of the two weighting schemes is similar, which is primarily due to the large correlation between the channels observed by the D symbols. The performance gains from optimal weighting are even more for PER (figure not shown).

VI. CONCLUSIONS

In this paper we analyzed receive AS with channel estimates that are affected both by noise and the time variations of the fading channel. For practical training (pilot) structures that are typical for AS systems, the channel estimates of different antenna elements are outdated by different amounts. We saw that this has important consequences for the selection criteria and the overall system performance. Our most important results and insights are the following: We proposed a new optimal selection scheme that weights the channel estimates before antenna selection. We derived closed-form expressions for the SEP for both MPSK and MQAM constellations in such a system, and derived the optimal weights to be used. The optimal weights are different from those suggested by MMSE prediction, and can significantly improve performance. We saw that increasing the number of antenna elements can worsen performance when unweighted AS is used. Optimum weighted selection could remedy this effect. We also considered uncoded and coded packet reception, in which the receiver is constrained in practice to use the same receive antenna to receive the entire packet. We found an approximate expression for the PER that was used to find the selection weights. The uncoded packet case also motivated other computationally efficient criteria for selecting the optimal antenna to minimize the PER. These criteria, which were motivated in different ways by the analytical results on SEP optimal weights, led to significant, but similar, improvements in the PER for both uncoded and coded packets. We believe that similar selection criteria carry over to antenna selection over frequency-selective channels, which is an interesting avenue for future work.

⁶We generate the genie-aided result by measuring, from simulations, the noise-averaged PER for each antenna, and then selecting the antenna with lowest PER. While this is computationally impractical, it provides a better benchmark than, for example, the perfect CSI case as the genie-aided receiver uses imperfect estimates for data decoding. Since the genie can measure PER at all the antennas of the receiver, it performs better than any practical scheme.

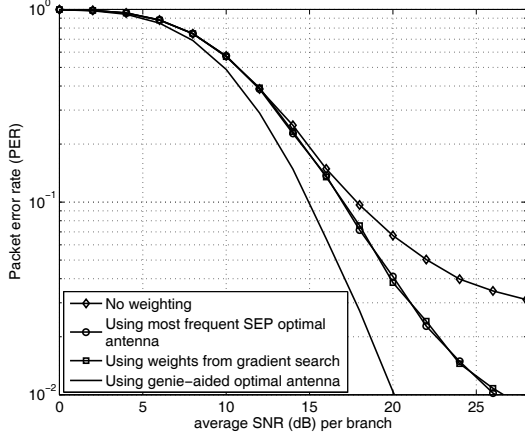


Fig. 9. Uncoded PER as a function of SNR for the two different weighted selection schemes of Sec. IV-C and Sec. IV-D (8PSK, $f_d T_p = 0.02$, $N = 4$, $T_p = 10T_s$, and $D = 10$).

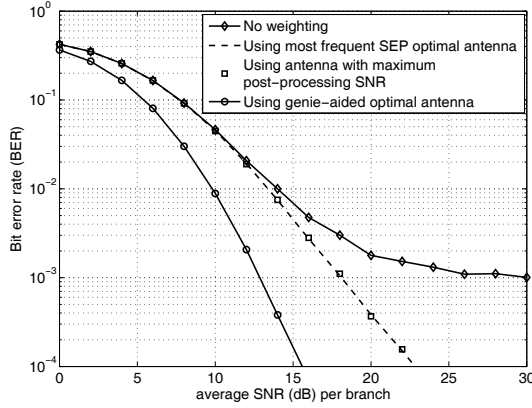


Fig. 10. Performance of weighted selection schemes for coded packet reception (8PSK, $f_d T_p = 0.01$, $T_p = 100T_s$, $D = 100$, and $N = 4$).

APPENDIX

A. Proof of Lemma 1

Note that e_k is independent of h_k but not \hat{h}_k . From (1), we can see that e_k , conditioned on \hat{h}_k , is a Gaussian RV. Hence, using standard results on conditional Gaussians, its first conditional moment is

$$\mathbf{E}[e_k | \hat{h}_k] = \mathbf{E}[e_k] + \frac{\text{Cov}(e_k, \hat{h}_k)}{\text{var}[\hat{h}_k]} (\hat{h}_k - \mathbf{E}[\hat{h}_k]), \quad (22)$$

where $\text{Cov}(\cdot, \cdot)$ denotes covariance. On substituting $\text{Cov}(e_k, \hat{h}_k) = \sigma_e^2$ and $\text{var}[\hat{h}_k] = 1 + \sigma_e^2$, we get

$$\mathbf{E}[e_k | \hat{h}_k] = \frac{\sigma_e^2}{1 + \sigma_e^2} \hat{h}_k = \hat{h}_k (1 - q^2). \quad (23)$$

From (5), \mathcal{D} depends only on the RVs $\hat{h}_{[\hat{1}]_i}$, $[\hat{1}]_i$, and s_i . Hence,

$$\begin{aligned} \mathbf{E}[\mathcal{D} | \{\hat{h}_k\}_{k=1}^N, s_i] &= \mathbf{E}[\mathcal{D} | \hat{h}_{[\hat{1}]_i}, [\hat{1}]_i, s_i], \\ &= |\hat{h}_{[\hat{1}]_i}|^2 \rho_{[\hat{1}]_i}^{(i)} s_i - \hat{h}_{[\hat{1}]_i}^* \rho_{[\hat{1}]_i}^{(i)} s_i \mathbf{E}[e_{[\hat{1}]_i} | \hat{h}_{[\hat{1}]_i}, [\hat{1}]_i], \\ &= |\hat{h}_{[\hat{1}]_i}|^2 \rho_{[\hat{1}]_i}^{(i)} s_i q^2. \end{aligned} \quad (24)$$

The first equality follows because both n'_k and n_k are independent of \hat{h}_k . The second equality directly follows from (23). Again using standard results on conditional Gaussians, we have

$$\begin{aligned} \text{var}[e_k | \hat{h}_k] &= \text{var}[e_k] - \frac{\text{Cov}(e_k, \hat{h}_k) (\text{Cov}(\hat{h}_k, e_k))^*}{\text{var}[\hat{h}_k]}, \\ &= q^2 \sigma_e^2. \end{aligned} \quad (25)$$

The expression in (7) then follows.

B. Proof of Theorem 1

The standard SEP expression for MPSK when \mathcal{D} is a Gaussian RV [31, (40)] is

$$P_i(\text{Err} | \{\hat{h}_k\}_{k=1}^N) = \frac{1}{\pi} \int_0^{\frac{M-1}{M}\pi} \exp\left(-\frac{|\mu_{\mathcal{D}}|^2 \sin^2(\frac{\pi}{M})}{\sigma_{\mathcal{D}}^2 \sin^2 \theta}\right) d\theta.$$

Making use of the results of Lemma 1, the above equation can be simplified to

$$P_i(\text{Err} | \{\hat{h}_k\}_{k=1}^N) = \frac{1}{\pi} \int_0^{\frac{M-1}{M}\pi} \exp\left(-\frac{|\hat{h}_{[\hat{1}]_i}|^2 b_{[\hat{1}]_i}^{(i)}}{\sin^2 \theta}\right) d\theta, \quad (26)$$

where $b_k^{(i)} \triangleq \frac{E_s |\rho_k^{(i)}|^2 q^4 \sin^2(\frac{\pi}{M})}{|\rho_k^{(i)}|^2 E_s \sigma_e^2 q^2 + N_0 + (1 - |\rho_k^{(i)}|^2) E_s}$. Expressing

q^2 and σ_e^2 in terms of γ , $b_k^{(i)}$ simplifies further to

$$b_k^{(i)} = \frac{|\rho_k^{(i)}|^2 \sin^2(\frac{\pi}{M})}{(1 + \frac{1}{\gamma \varepsilon}) (\varepsilon (1 - |\rho_k^{(i)}|^2) + \frac{1 + \varepsilon}{\gamma} + \frac{1}{\gamma^2})}.$$

Averaging over the selected antenna index, we get

$$\begin{aligned} P_i(\text{Err} | \{\hat{h}_k\}_{k=1}^N) &= \sum_{m=1}^N \Pr([\hat{1}]_i = m | \{\hat{h}_k\}_{k=1}^N) P_i(\text{Err} | \{\hat{h}_k\}_{k=1}^N, [\hat{1}]_i = m), \\ &= \frac{1}{\pi} \sum_{m=1}^N \left[\prod_{\substack{l=1 \\ l \neq m}}^N \Pr(w_l |\hat{h}_l|^2 < w_m |\hat{h}_m|^2 | \{\hat{h}_k\}_{k=1}^N) \right] \\ &\quad \times \int_0^{\frac{M-1}{M}\pi} \exp\left(-\frac{|\hat{h}_m|^2 b_m^{(i)}}{\sin^2 \theta}\right) d\theta. \end{aligned}$$

From (1), the probability density function, $f(x)$, and the cumulative distribution function, $F(x)$, of $|\hat{h}_k|^2$ are given

by $f(x) = \frac{1}{1+\sigma_e^2} \exp\left(\frac{-x}{1+\sigma_e^2}\right)$ and $F(x) = 1 - \exp\left(\frac{-x}{1+\sigma_e^2}\right)$. Therefore, the SEP averaged over $\{\hat{h}_k\}_{k=1}^N$ equals

$$P_i(\text{Err}) = \frac{1}{\pi} \sum_{m=1}^N \int_0^\infty \int_0^{\frac{M-1}{M}\pi} \exp\left(\frac{-xb_m^{(i)}}{\sin^2\theta}\right) \times f(x) \prod_{\substack{l=1 \\ l \neq m}}^N F\left(\frac{w_l x}{w_l}\right) d\theta dx. \quad (27)$$

The term $\prod_{\substack{l=1 \\ l \neq m}}^N F\left(\frac{w_l x}{w_l}\right)$ in the integrand above, when expanded, takes the following form [26]:

$$\sum_{r=0}^{N-1} \frac{(-1)^r}{r!} \sum_{\substack{l_0, \dots, l_r=1 \\ l_0=1, l_1 \neq \dots \neq l_r \neq m}}^N \exp\left(\frac{-x \left(\sum_{j=1}^r \frac{w_m}{w_{l_j}}\right)}{1 + \sigma_e^2}\right).$$

Consequently, the SEP expression in (27) simplifies to:

$$P_i(\text{Err}) = \frac{1}{\pi (1 + \sigma_e^2)} \sum_{m=1}^N \sum_{r=0}^{N-1} \sum_{\substack{l_0, \dots, l_r=1 \\ l_0=1, l_1 \neq \dots \neq l_r \neq m}}^N \frac{(-1)^r}{r!} \times \int_0^{\frac{M-1}{M}\pi} \left(\frac{b_m^{(i)}}{\sin^2\theta} + \frac{1 + \sum_{j=1}^r \frac{w_m}{w_{l_j}}}{1 + \sigma_e^2} \right)^{-1} d\theta. \quad (28)$$

The single integral above can be eliminated using the following identity, which follows from [26, 2.562]. For $a, b > 0$,

$$\int_0^\zeta \left(\frac{a}{\sin^2\theta} + b \right)^{-1} d\theta \equiv \frac{1}{b} \left[\zeta - \sqrt{\frac{a}{a+b}} \tan^{-1} \left(\sqrt{\frac{a+b}{a}} \tan \zeta \right) \right]. \quad (29)$$

C. Proof of Theorem 2

The standard MQAM SEP expression when \mathcal{D} is a Gaussian RV is⁷ [31, (48)]

$$P_i(\text{Err}\{\hat{h}_k\}_{k=1}^N) = \frac{4}{\pi} \left(1 - \frac{1}{\sqrt{M}}\right) \int_0^{\frac{\pi}{2}} \exp\left(\frac{-1.5 |\mu_{\mathcal{D}}|^2 / \sigma_{\mathcal{D}}^2}{(M-1) \sin^2\theta}\right) d\theta - \frac{4}{\pi} \left(1 - \frac{1}{\sqrt{M}}\right)^2 \int_0^{\frac{\pi}{4}} \exp\left(\frac{-1.5 |\mu_{\mathcal{D}}|^2 / \sigma_{\mathcal{D}}^2}{(M-1) \sin^2\theta}\right) d\theta. \quad (30)$$

From Lemma 1, the above equation can be simplified to

$$P_i(\text{Err}\{\hat{h}_k\}_{k=1}^N) = \frac{4}{\pi} \left(1 - \frac{1}{\sqrt{M}}\right) \int_0^{\frac{\pi}{2}} \exp\left(\frac{-|\hat{h}_{[1]_i}|^2 c_{[1]_i}^{(i)}}{\sin^2\theta}\right) d\theta - \frac{4}{\pi} \left(1 - \frac{1}{\sqrt{M}}\right)^2 \int_0^{\frac{\pi}{4}} \exp\left(\frac{-|\hat{h}_{[1]_i}|^2 c_{[1]_i}^{(i)}}{\sin^2\theta}\right) d\theta, \quad (31)$$

⁷The derivation of this expression assumes that the variance of \mathcal{D} is the same for all symbols of the MQAM constellation. With imperfect estimation, this is no longer the case, as can be seen from (7). However, as the simulation results in [16] and this paper show, the approximation is accurate.

where $c_k^{(i)} = \frac{\varepsilon |\rho_k^{(i)}|^2 \left(\frac{1.5}{M-1}\right)}{(1 + \frac{1}{\gamma\varepsilon}) \left(\varepsilon \left(1 - |\rho_k^{(i)}|^2\right) + \frac{1+\varepsilon}{\gamma} + \frac{1}{\gamma^2}\right)}$. Along the lines of Appendix B, we can show that

$$\mathbf{E} \left[\int_0^\psi \exp\left(\frac{-|\hat{h}_{[1]_i}|^2 b_{[1]_i}^{(i)}}{\sin^2\theta}\right) d\theta \right] = \sum_{k=1}^N \sum_{r=0}^{N-1} \sum_{\substack{l_0, \dots, l_r=1 \\ l_0=1, l_1 \neq \dots \neq l_r \neq k}}^N \left\{ 1 + \sum_{j=1}^r \frac{w_k}{w_{l_j}} \right\}^{-1} \times \frac{(-1)^r}{r!} \left[\psi - \frac{\tan^{-1} \left(\sqrt{\alpha_k^{(i)}(\gamma, w_{l_1}, \dots, w_{l_r})} \tan \psi \right)}{\sqrt{\alpha_k^{(i)}(\gamma, w_{l_1}, \dots, w_{l_r})}} \right],$$

where $\alpha_m^{(i)}(\gamma, w_{l_1}, \dots, w_{l_r})$ is defined in (9), the expectation is taken over the channel estimates $\{\hat{h}_k\}_{k=1}^N$, and ψ is either $\frac{\pi}{4}$ or $\frac{\pi}{2}$. Hence, each of the two integrals in (31) simplifies to

$$\mathbf{E} \left[\int_0^\psi \exp\left(\frac{-|\hat{h}_{[1]_i}|^2 c_{[1]_i}^{(i)}}{\sin^2\theta}\right) d\theta \right] = \sum_{k=1}^N \sum_{r=0}^{N-1} \sum_{\substack{l_0, \dots, l_r=1 \\ l_0=1, l_1 \neq \dots \neq l_r \neq k}}^N \left\{ 1 + \sum_{j=1}^r \frac{w_k}{w_{l_j}} \right\}^{-1} \times \frac{(-1)^r}{r!} \left[\psi - \frac{\tan^{-1} \left(\sqrt{\beta_k^{(i)}(\gamma, w_{l_1}, \dots, w_{l_r})} \tan \psi \right)}{\sqrt{\beta_k^{(i)}(\gamma, w_{l_1}, \dots, w_{l_r})}} \right],$$

where $\beta_m^{(i)}(\gamma, w_{l_1}, \dots, w_{l_r})$ is defined in (11). Substituting this in (31) yields the desired result.

D. Proof of Theorem 3

We now give proof for the optimal selection weights, which uses physical arguments. It will also prove that linear weighting is indeed the SEP optimal selection strategy among all possible selection strategies. Let antenna k be selected and used for data reception. For MQAM, (31) can be rewritten as

$$P_i(\text{Err}\{\hat{h}_k\}) = \frac{4}{\pi} \left(1 - \frac{1}{\sqrt{M}}\right) \int_0^{\frac{\pi}{2}} \xi(\theta) \exp\left(\frac{-|\hat{h}_k|^2 c_k^{(i)}}{\sin^2\theta}\right) d\theta, \quad (32)$$

where $\xi(\theta) = 1/\sqrt{M}$, for $0 \leq \theta < \pi/4$, and $\xi(\theta) = 1$, for $\pi/4 \leq \theta \leq \pi/2$. From this special form of the SEP, it follows that the minimum SEP obtained by selecting the best antenna equals

$$\frac{4}{\pi} \left(1 - \frac{1}{\sqrt{M}}\right) \int_0^{\frac{\pi}{2}} \xi(\theta) \min_{k=1, \dots, N} \exp\left(\frac{-|\hat{h}_k|^2 c_k^{(i)}}{\sin^2\theta}\right) d\theta. \quad (33)$$

It is important to note that (31) and (33) hold for any selection strategy – they do not assume linear weighted selection. Thus, the optimal antenna to use for data reception is the one that

maximizes $\arg \max_k \left(|\hat{h}_k|^2 c_k^{(i)} \right)$, which shows that linear weighting is the optimal strategy and that the optimal weights are as stated in the theorem. A similar argument works for MPSK since (26) can be written in a form similar to (32) as

$$P_i(\text{Err}|\hat{h}_k) = \frac{1}{\pi} \int_0^{\frac{M-1}{M}\pi} \exp\left(\frac{-|\hat{h}_k|^2 b_k^{(i)}}{\sin^2 \theta}\right) d\theta. \quad (34)$$

An alternate proof that exploits the symmetry inherent in the SEP expression to show that $\left. \frac{\partial}{\partial w_p} P_i^{\text{MPSK}}(\gamma) \right|_{\{w_{k,i}\}_{k=1}^N = \{w_{k,i}^{\text{opt}}\}_{k=1}^N} = 0$ is given in [32].

E. Proof of Lemma 2

Using (29), the inner most integral in (17) reduces to

$$\int_0^{\frac{M-1}{M}\pi} \left(\sum_{k=1}^n \frac{a_k}{\sin^2 \theta_k} + b \right)^{-1} d\theta_1 = \left(\sum_{k=2}^n \frac{a_k}{\sin^2 \theta_k} + b \right)^{-1} \times \left[\frac{M-1}{M}\pi - \frac{1}{z_2} \tan^{-1} \left(z_2 \tan \left(\frac{M-1}{M}\pi \right) \right) \right],$$

with $z_2 \triangleq \frac{\sum_{k=2}^n \frac{a_k}{\sin^2 \theta} + a_1 + b}{a_1}$. Since $\sin^2(\theta) \leq 1$, it easily follows that $z_2 \geq \frac{\sum_{k=1}^n a_k + b}{a_1}$. For $M > 2$, $\tan\left(\frac{M-1}{M}\pi\right) < 0$. Hence, $z_2 \tan\left(\frac{M-1}{M}\pi\right) \leq \frac{\sum_{k=1}^n a_k + b}{a_1} \tan\left(\frac{M-1}{M}\pi\right)$. This results in

$$\frac{M-1}{M}\pi - \frac{1}{z_2} \tan^{-1} \left(z_2 \tan \left(\frac{M-1}{M}\pi \right) \right) \geq \tau_1,$$

where τ_k is defined in theorem statement. (For $M = 2$, the above inequality is trivially satisfied since $\tan\left(\frac{\pi}{2}\right) = \infty$.) Hence, for $M \geq 2$,

$$\int_0^{\frac{M-1}{M}\pi} \left(\sum_{k=1}^n \frac{a_k}{\sin^2 \theta_k} + b \right)^{-1} d\theta_1 \geq \tau_1 \left(\sum_{k=2}^n \frac{a_k}{\sin^2 \theta_k} + b \right)^{-1}.$$

Using the above identity recursively, the n -dimensional integral can be simplified as follows:

$$\begin{aligned} & \int_{\theta_n=0}^{\frac{M-1}{M}\pi} \cdots \int_{\theta_1=0}^{\frac{M-1}{M}\pi} \left(\sum_{k=1}^n \frac{a_k}{\sin^2 \theta_k} + b \right)^{-1} d\theta_1 \cdots d\theta_n \\ & \geq \tau_1 \int_{\theta_n=0}^{\frac{M-1}{M}\pi} \cdots \int_{\theta_2=0}^{\frac{M-1}{M}\pi} \left(\sum_{k=2}^n \frac{a_k}{\sin^2 \theta_k} + b \right)^{-1} d\theta_2 \cdots d\theta_n \\ & \geq \cdots \geq \frac{1}{b} \prod_{k=1}^n \tau_k. \end{aligned}$$

REFERENCES

- [1] A. F. Molisch and M. Z. Win, "MIMO systems with antenna selection," *IEEE Microwave Mag.*, vol. 5, pp. 46–56, Mar. 2004.
- [2] S. Sanayei and A. Nosratinia, "Antenna selection in MIMO systems," *IEEE Commun. Mag.*, pp. 68–73, Oct. 2004.
- [3] N. B. Mehta and A. F. Molisch, "Antenna selection in MIMO systems," in *MIMO System Technology for Wireless Communications* (G. Tsoulos, ed.), ch. 6, CRC Press, 2006.
- [4] A. Ghayeb and T. M. Duman, "Performance analysis of MIMO systems with antenna selection over quasi-static fading channels," *IEEE Trans. Veh. Technol.*, vol. 52, pp. 281–288, Mar. 2003.

- [5] D. A. Gore and A. Paulraj, "MIMO antenna subset selection with space-time coding," *IEEE Trans. Signal Process.*, vol. 50, pp. 2580–2588, Oct. 2002.
- [6] A. Gorokhov, D. Gore, and A. Paulraj, "Receive antenna selection for MIMO flat-fading channels: Theory and algorithms," *IEEE Trans. Inf. Theory*, vol. 49, pp. 2687–2696, 2003.
- [7] A. B. Narasimhamurthy and C. Tepedelenlioglu, "Antenna selection for MIMO OFDM systems with channel estimation error," in *Proc. Globecom*, pp. 3290–3294, 2007.
- [8] "Draft amendment to wireless LAN media access control (MAC) and physical layer (PHY) specifications: Enhancements for higher throughput," Tech. Rep. P802.11n/D0.04, IEEE, Mar. 2006.
- [9] "Technical specification group radio access network; evolved universal terrestrial radio access (E-UTRA); physical layer procedures (release 8)," Tech. Rep. 36.211 (v8.3.0), 3rd Generation Partnership Project (3GPP), 2008.
- [10] N. B. Mehta, A. F. Molisch, J. Zhang, and E. Bala, "Antenna selection training in MIMO-OFDM/OFDMA cellular systems," in *IEEE CAM-SAP*, 2007.
- [11] X. N. Zeng and A. Ghayeb, "Performance bounds for space-time block codes with receive antenna selection," *IEEE Trans. Inf. Theory*, vol. 50, pp. 2130–2137, Sept. 2004.
- [12] M. Z. Win and J. H. Winters, "Virtual branch analysis of symbol error probability for hybrid selection/maximal-ratio combining in Rayleigh fading," *IEEE Trans. Commun.*, vol. 49, pp. 1926–1934, Nov. 2001.
- [13] Z. Chen, J. Yuan, and B. Vucetic, "Analysis of transmit antenna selection/maximal-ratio combining in Rayleigh fading channels," *IEEE Trans. Veh. Technol.*, vol. 54, pp. 1312–1321, Jul. 2005.
- [14] Z. Xu, S. Sfar, and R. S. Blum, "Analysis of MIMO systems with receive antenna selection in spatially correlated Rayleigh fading channels," *IEEE Trans. Veh. Technol.*, vol. 58, pp. 251–262, Jan. 2009.
- [15] H. Zhang, A. Molisch, and J. Zhang, "Applying antenna selection in WLANs for achieving broadband multimedia communications," *IEEE Trans. Broadcast.*, vol. 52, pp. 475–482, Dec. 2006.
- [16] W. M. Gifford, M. Z. Win, and M. Chiani, "Antenna subset diversity with non-ideal channel estimation," *IEEE Trans. Wireless Commun.*, vol. 7, pp. 1527–1539, May 2008.
- [17] P. Theofilakos and A. G. Kanatas, "Robustness of receive antenna subarray formation to hardware and signal non-idealities," in *Proc. VTC (Spring)*, pp. 324–328, 2007.
- [18] K. Zhang and Z. Niu, "Adaptive receive antenna selection for orthogonal space-time block codes with channel estimation errors with antenna selection," in *Proc. Globecom*, pp. 3314–3318, 2005.
- [19] J. Tang, X. Zhang, and Q. Du, "Alamouti scheme with joint antenna selection and power allocation over Rayleigh fading channels in wireless networks," in *Proc. Globecom*, pp. 3319–3323, 2005.
- [20] T. Gucluoglu and E. Panayirci, "Performance of transmit and receive antenna selection in the presence of channel estimation errors," *IEEE Commun. Lett.*, vol. 12, pp. 371–373, May 2008.
- [21] S. Han and C. Yang, "Performance analysis of MRT and transmit antenna selection with feedback delay and channel estimation error," in *Proc. WCNC*, pp. 1135–1139, 2007.
- [22] W. Xie, S. Liu, D. Yoon, and J.-W. Chong, "Impacts of Gaussian error and Doppler spread on the performance of MIMO systems with antenna selection," in *Proc. Int. Conf. Wireless. Commun., Netw., Mobile Comput.*, pp. 1–4, 2006.
- [23] V. Kristem and N. B. Mehta, "Receive antenna selection with imperfect channel knowledge from training," in *Proc. Nat. Conf. Commun.*, 2009.
- [24] A. F. Molisch, *Wireless Communications*. Wiley-IEEE Press, 2005.
- [25] D. V. Marathe and S. Bhashyam, "Power control for multi-antenna Gaussian channels with delayed feedback," in *Proc. Asilomar Conf. on Signals, Syst., and Comput.*, pp. 1598–1602, 2005.
- [26] L. S. Gradshteyn and L. M. Ryzhik, *Tables of Integrals, Series and Products*. Academic Press, 2000.
- [27] C. Tepedelenlioglu, A. Abdi, G. B. Giannakis, and M. Kaveh, "Estimation of Doppler spread and signal strength in mobile communications with applications to handoff and adaptive transmission," *Wireless Commun. and Mobile Computing*, vol. 1, pp. 221–242, 2001.
- [28] A. Dogandzic and B. Zhang, "Estimating Jakes' Doppler power spectrum parameters using the Whittle approximation," *IEEE Trans. Signal Process.*, vol. 53, pp. 987–1005, Mar. 2005.
- [29] Y. Li and Y. Guan, "Modified Jakes model for simulating multiple uncorrelated fading waveforms," in *Proc. ICC*, pp. 46–49, 2000.
- [30] "Technical specification group radio access network; evolved universal terrestrial radio access (E-UTRA); multiplexing and channel coding (release 8)," Tech. Rep. 36.212 (v8.2.0), 3rd Generation Partnership Project (3GPP), 2008.

- [31] M.-S. Alouini and A. Goldsmith, "A unified approach for calculating error rates of linearly modulated signals over generalized fading channels," *IEEE Trans. Commun.*, vol. 47, pp. 1324–1334, Sept. 1999.
- [32] V. Kristem, N. B. Mehta, and A. F. Molisch, "Optimal weighted antenna selection for imperfect channel knowledge from training," in *Proc. ICC*, 2009.

PLACE
PHOTO
HERE

Andreas F. Molisch (S'89, M'95, SM'00, F'05) received the Dipl. Ing., Dr. techn., and habilitation degrees from the Technical University Vienna (Austria) in 1990, 1994, and 1999, respectively. From 1991 to 2000, he was with the TU Vienna, becoming an associate professor there in 1999. From 2000–2002, he was with the Wireless Systems Research Department at AT&T (Bell) Laboratories Research in Middletown, NJ. From 2002–2008, he was with Mitsubishi Electric Research Labs, Cambridge, MA, USA, most recently as Distinguished Member of Technical Staff and Chief Wireless Standards Architect. Concurrently he was also Professor and Chairholder for radio systems at Lund University, Sweden. Since 2009, he is Professor of Electrical Engineering at the University of Southern California, Los Angeles, CA, USA.

Dr. Molisch has done research in the areas of SAW filters, radiative transfer in atomic vapors, atomic line filters, smart antennas, and wideband systems. His current research interests are measurement and modeling of mobile radio channels, UWB, cooperative communications, and MIMO systems. Dr. Molisch has authored, co-authored or edited four books (among them the textbook "Wireless Communications, Wiley-IEEE Press), eleven book chapters, some 130 journal papers, and numerous conference contributions, as well as more than 70 patents.

Dr. Molisch is an Area editor of the IEEE Trans. Wireless Commun. for Antennas and Propagation and co-editor of special issues of several journals. He has been member of numerous TPCs, vice-chair of the TPCs of VTC 2005 spring and VTC 2010 spring, general chair of ICUWB 2006, TPC co-chair of the wireless symposium of Globecom 2007, TPC chair of Chinacom2007, general chair of Chinacom 2008, TPC co-chair of the Commun. Theory Workshop 2009, tutorial co-chair of WCNC 2009, and workshop co-chair at ICC 2010. He has participated in the European research initiatives "COST 231", "COST 259", and "COST273", where he was chairman of the MIMO channel working group, he was chairman of the IEEE 802.15.4a channel model standardization group. From 2005–2008, he was also chairman of Commission C (signals and systems) of URSI (International Union of Radio Scientists), and since 2009, he is the Chair of the Radio Communications Committee of the IEEE Communications Society. Dr. Molisch is a Fellow of the IEEE, a Fellow of the IET, an IEEE Distinguished Lecturer, and recipient of several awards.

PLACE
PHOTO
HERE

Vinod Kristem Vinod Kristem received his Bachelor of Technology degree in Electronics and Communications Engineering from the National Institute of Technology (NIT), Warangal in 2007. He received his Master of Engineering degree in Telecommunications from Indian Institute of Science, Bangalore, India in 2009. Since then, he was with Beceem Communications Pvt Ltd, Bangalore, India, working on channel estimation and physical layer measurements for WiMAX and LTE. His research interests include the design and analysis of algorithms for wireless

communication networks, MIMO systems, and cooperative communications.

PLACE
PHOTO
HERE

Neelesh B. Mehta (S'98-M'01-SM'06) received his Bachelor of Technology degree in Electronics and Communications Engineering from the Indian Institute of Technology (IIT), Madras in 1996, and his M.S. and Ph.D. degrees in Electrical Engineering from the California Institute of Technology, Pasadena, CA in 1997 and 2001, respectively. He was a visiting graduate student researcher at Stanford University in 1999 and 2000. He is now an Assistant Professor at the Dept. of Electrical Communication Engineering, Indian Institute of Science

(IISc), Bangalore, India. Until 2002, he was a research scientist in the Wireless Systems Research group in AT&T Laboratories, Middletown, NJ. In 2002–2003, he was a Staff Scientist at Broadcom Corp., Matawan, NJ, and was involved in GPRS/EDGE cellular handset development. From 2003–2007, he was a Principal Member of Technical Staff at the Mitsubishi Electric Research Laboratories, Cambridge, MA, USA.

His research includes work on link adaptation, multiple access protocols, WCDMA downlinks, system-level performance analysis of cellular systems, MIMO and antenna selection, and cooperative communications. He was also actively involved in radio access network physical layer (RAN1) standardization activities in 3GPP. He has served on several TPCs, and was a TPC co-chair for WISARD 2010, the Transmission technologies track of VTC 2009 (Fall), and the Frontiers of Networking and Communications symposium of Chinacom 2008. He is an Editor of the IEEE Transactions on Wireless Communications and an executive committee member of the IEEE Bangalore Section and the Bangalore chapter of the IEEE Signal Processing Society.